

# Effect of vibration on the critical state of dry granular soils

Karen A. Taslagyan<sup>1</sup> · Dave H. Chan<sup>1</sup> · Norbert R. Morgenstern<sup>1</sup>

Received: 29 October 2014 / Published online: 3 September 2015  
© Springer-Verlag Berlin Heidelberg 2015

**Abstract** In order to investigate the effect of vibration on the critical state of dry granular soils, eighty samples of four different granular materials were tested at four normal stresses under different vibrational accelerations. The experiments were performed on a modified vibrational direct shear apparatus with vibrational loading in the horizontal (shear) direction. Strength loss versus vibration acceleration plots at different normal stresses, as well as the peak, residual and vibro-residual shear strength diagrams have been obtained for the four granular materials at different intensities of vibration. It has been determined that increasing the intensity of vibration reduces the friction angle of the granular materials. The effect of particle shape on the strength loss due to vibration has been observed as well as the effect of vibration on the normal stress.

**Keywords** Vibration · Shear strength · Granular soils · Critical state · Friction angle

## 1 Introduction

Granular soils are frequently exposed to vibrations due to earthquakes, blasting, construction operations, machinery and vehicle traffic vibrations. The strength behavior of a soil during vibration depends not only on the vibration characteristics, such as acceleration, frequency and amplitude, but

also on the physical properties of the soil such as moisture content, grain size distribution, particle shape, dry density or void ratio, density and mineralogy of soil particles, cohesion and internal friction angle.

There has been significant progress in understanding the effects of vibration on the strength and deformation properties of soils since the first half of the last century [2, 8, 9, 12, 24, 30, 31]. A number of different experiments with vibration application have been conducted on cohesive and cohesionless soils that generated very valuable data leading to some important conclusions [16, 22, 25, 26, 28, 35]. All these findings help to improve the design of different structures subjected to dynamic loads significantly [2, 5, 24, 27, 29, 30].

Despite the knowledge gained on this issue in the last few decades, there is still a lack of understanding on the mechanism of particle interactions and shear deformation due to vibration. Therefore, there is a need to study the shear strength and deformation behavior of soils due to vibrations. In particular it is specifically interesting to determine the effect of vibration on the residual shear strength of soils, that is, the effect of vibration on the critical state, a unique state independent of the initial density (void ratio) of the soil that can be reached upon sufficiently large shear deformations.

If large displacements are anticipated, the design of a structure, such as an earth or tailing dam, has to take into account the residual shear strength characteristics of the soils underlying or/and constituting the structure. In this case, if the soil is subjected to vibrations, depending on the magnitude of vibration, it may undergo some loss of strength resulting in excessive deformations and compromising the stability of the structure. Therefore, it is of paramount importance to predict and consider the effects of vibrations on the residual strength of soils.

✉ Karen A. Taslagyan  
taslagya@ualberta.ca

Dave H. Chan  
dave.chan@ualberta.ca

Norbert R. Morgenstern  
norbert.morgenstern@ualberta.ca

<sup>1</sup> University of Alberta, Edmonton, Canada

## 2 Previous studies on vibrational loading on soils

There are two important aspects that contribute to the unique properties of granular materials: ordinary variation in temperature plays no role on the mechanical response of the material, and the interactions between grains are dissipative because of static friction and the inelasticity of collisions [14]. Pokrovsky [21] was the first to investigate experimentally the influence of vibrations on the internal friction of sand. He showed that the coefficient of internal friction depends on the kinetic energy of vibration. As the energy increases, the coefficient decreases, approaching a value 25–30 % smaller than that observed before vibration. These results were later supported by experiments performed by Barkan [2], who tested sand at vibration frequency of  $140 \text{ s}^{-1}$  and amplitude of 0.5–0.15 mm. It is concluded that vibration has considerable effects on the shearing resistance of soil and the internal friction is lower than the static friction during vibration. Increase in acceleration will decrease the internal friction approaching asymptotically to a limit value which depends on the properties of a soil. Analogous experiments conducted on sand having 10–12 % moisture content showed that the moist sand subjected to vibration had smaller decrease in the internal friction than dry sand. This was attributed to the capillary forces between soil particles with 10–12 % moisture content.

Additional confirmation of the above observations was provided by Savchenko [28] who revealed that at a constant vibrational frequency, the coefficient of internal friction of sand decreases continuously as the amplitude increases. The dependence of  $\tan \varphi$  on the frequency of vibration is more complicated, and as the test results showed, there exist frequency ranges corresponding to small and large changes in  $\tan \varphi$  of sand. Savchenko also tested two sets of medium grained sand at different moisture contents (2–24 %), constant vibration amplitude 0.35 mm and two vibration frequencies of 144 and  $250 \text{ s}^{-1}$ , respectively. For both sets of samples the largest decrease in  $\tan \varphi$  was observed at approximately 13 % moisture content [2]. Barkan [2] concluded that the principal vibration parameter which determines the effect of vibrations and shocks on the compaction of soils is the acceleration, or rather the inertial force, which acts on the soil particles during vibration. Metcalfe et al. [20] and Huan [10] also confirm that the dimensionless acceleration  $\Gamma = A \omega^2/g$  is a key vibration parameter, where  $A$  is vibration amplitude,  $\omega$ —frequency and  $g$ —gravitational acceleration.

To study the influence of particle size on the effect of vibration, Savchenko conducted experiments on four different sizes of sand at vibrational frequencies of 144 and  $250 \text{ s}^{-1}$  and constant vibration amplitude of 0.35 mm [2]. The results revealed that the effect of vibration on internal friction in sand is directly proportional to the diameter of the sand grains [2]. On the other hand, Maslov [15] performed a series of experi-

ments on sands and concluded that vibration did not cause any changes in the coefficient of internal friction of sand, and that the changes in its shear resistance were due to a decrease in the normal stress caused by vibration. Shibata and Yukitomo [32] carried out drained triaxial vibrating tests. The results revealed that the dynamic strength increased with the increasing of the density of sand, and that the influence of vibration frequency on the strength of sand was rather remarkable, the higher the frequency, the lower the shear strength.

An interesting concept of “Dynamic fluidization” was proposed by Richards et al. [23]. They considered the effect of earthquake accelerations on dry granular soils. It is hypothesized that the imposed accelerations at some critical level changes the state of the soil, causing general plastification, such that the soil becomes, in a sense, an anisotropic fluid. It is assumed that the main trigger of fluidization is the inertial forces acting between the particles of a granular soil. It is shown that fluidization depends mainly on horizontal accelerations, not vertical accelerations. Another distinguishing feature of fluidization is that when it occurs, flow takes place, if at all, in finite increments rather than continuously, with the increments corresponding to the acceleration pulses of an earthquake above a critical value.

The authors distinguish three stages of dynamic fluidization: initial, intermediate and general. Initial fluidization is recognised as a threshold above which significant loss of soil shearing resistance may occur. For a dry sand at its neutral condition  $K_0$  initial fluidization takes place at  $\Gamma < 0.3$  and at even lower values for soils having smaller friction angle. For saturated loose granular soils, it is postulated that the initial fluidization will initiate liquefaction because of collapse of the soil structure under shear flow. At intermediate dynamic fluidization stage, the soil continues to lose its shearing resistance and provide support of the external loads from internal shearing generated by the inertial forces. When soil reaches the general dynamic fluidization stage, its shear strength is mobilized on a broad range of orientations, and the soil within these directions behaves like a viscous fluid [23].

Youd [37] performed laboratory experiments by mounting a direct shear apparatus on a shaking table to show the effects of vibration on the shear strength and void ratio of dry granular materials. It was concluded that each vibratory equilibrium void ratio<sup>1</sup> was also the critical void ratio when the sample was sheared under the same vibration. The critical void ratio and coefficient of internal friction both were reduced considerably during vibration.

Dijksman et al. [7] conducted experiments using a split-bottom shear cell, in which a layer of glass beads (1–1.3 mm diameter) having 18 mm depth was driven by the rotation of a rough disk of radius  $R_s = 4 \text{ cm}$  mounted flush with the bot-

<sup>1</sup> Vibratory equilibrium void ratio is defined as the ultimate minimum void ratio for a sample densified at a particular vibration.

tom. The shear cell was vibrated vertically and sinusoidally with frequency,  $f$ , and amplitude,  $A$ .  $f = 63 \text{ Hz}$  and  $\Gamma$  varied from 0 to 1 ( $\Gamma = A(2\pi f)^2/g$ ). It was established that the rheological curve of dry granular media is non-monotonic, both in the presence and absence of vibration. In the presence of weak vibrations, the non-monotonic flow curves govern a hysteretic transition between slow but steady and fast, inertial flows. In the absence of vibrations, the non-monotonic flow curve governs the yielding behavior of granular media.

Of special interest are the theories of “Mechanical fluidization” [6] and “Acoustic fluidization” [18] attempting to explain the large runout distance of big rock avalanches. The essence of mechanical fluidization is the concept that high energy input into a granular mass causes high impulsive contact pressures between individual grains such that they become statistically separated and the mass dilates. The internal shearing resistance is thereby reduced as shown by Bagnold [1] and Bjerrum et al. [3], and the mass may flow under gravity when dilated. The high relative velocity between the base of the high-speed debris flow and the bedding material of the flow channel causes high speed shearing with high energy resulting in dilation as shown by Bagnold [1] for a granular material subjected to unidirectional shearing [6]. On the other hand, Hungr [11] conducted high velocity ring shear experiments and did not observe any effect of “mechanical fluidization”. Several types of materials were tested, including two sizes of relatively coarse sand, mixtures of sand and rock flour, polystyrene beads and sand in water. All of these materials have been tested under different velocities and normal stresses. All exhibited straight linear residual strength envelopes with zero cohesion and unique angles of residual friction, practically unaffected by the speed of shearing [11].

The acoustic fluidization theory proposed by Melosh [18] is another attempt to explain the large runout distance of

sturzstroms observed on earth, as well as on the moon and Mars. Based on this theory, a thin layer of material can be fluidized by strong enough sound waves at the bottom interface of the moving debris, if its volume is large enough to retain enough acoustic energy to maintain fluidization. An important aspect of the flow process is that sound (acoustic energy) is created as the debris moves, and that the sound must have short wave-lengths compared to the dimensions of the fluidized rock debris. Melosh [19] also suggested that the overburden pressure at some faults can be relieved by means of acoustic fluidization and allow it to slide at low average stress [18]. Later Sornette and Sornette [33] found an inconsistency in Melosh’s theory of acoustic fluidization in explaining fault motion but acknowledged that the relevance of acoustic fluidization still remains an open question.

As it is seen from the studies mentioned above, nowadays there is no comprehensive model that can fully explain the mechanism of the effect of vibrations on the shear strength characteristics of soils. Moreover, some of the findings seem to contradict each other. Therefore, the shear strength characteristics of soils under the influence of vibrations remains an open subject.

### 3 Testing equipment and procedures

In order to investigate the effects of vibration on the residual shear strength of granular material, a direct shear apparatus was modified into a vibrational direct shear apparatus [34] as shown in Figs. 1 and 2. The modifications include installation of an electromagnetic actuator (11) between the proving ring (3) and the shear box (2), as well as two load cells (10 and 12) to measure the shear forces at the top and bottom halves of the shear box (2). An extension (13) of the main body (5) is

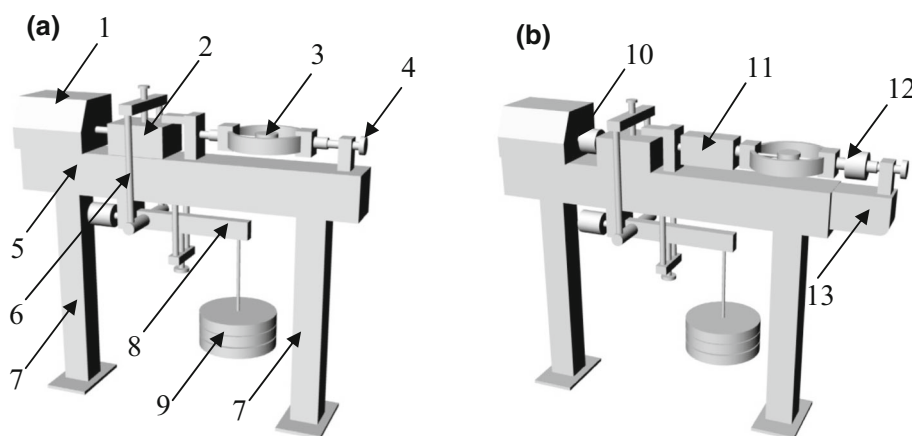


**Fig. 1** **a** Conventional strain controlled direct shear apparatus and **b** modified strain controlled vibrational direct shear apparatus; where: 1 control box of the direct shear apparatus; 2 shear box for soil sample; 3 proving ring; 4 screw for zero setting of shear load before starting a test; 5 main body of the direct shear apparatus; 6 frame for transferring

normal load to the soil sample placed in the shear box (2); 7 legs of the direct shear apparatus supporting the main body (5); 8 lever system to provide normal load to the soil sample; 9 weights to apply the normal load; 10 load cell; 11 actuator; 12 load cell; 13 extension of the main body (5) of the direct shear apparatus to accommodate the actuator

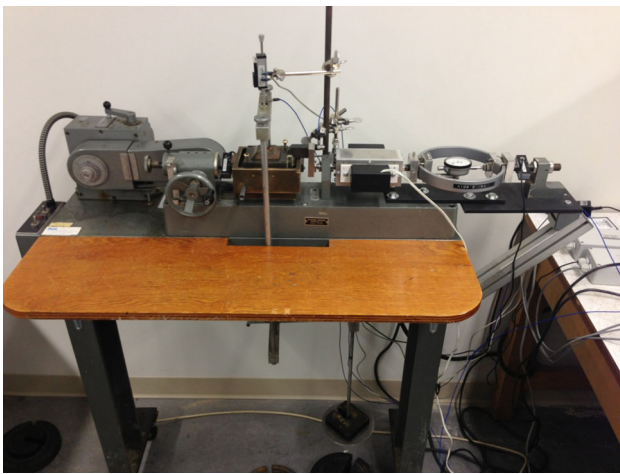


**Fig. 2** Photograph of the modified direct shear apparatus

**Table 1** Physical characteristics of the glass beads and sands

Material	Particle density $\rho_s$ (g/cm <sup>3</sup> )	Dry density $\rho$ (g/cm <sup>3</sup> )	Void ratio $e$	Porosity $n$
Glass beads 0.1 mm	2.65	1.49	0.779	0.438
Glass beads 0.5 mm	2.65	1.566	0.692	0.409
Fine sand	2.65	1.46	0.815	0.449
Coarse sand	2.65	1.755	0.510	0.338

needed to accommodate the actuator (11). The actuator (11) consists of two electromagnets, and the frequency and force can be changed by a control panel. The vibration generated by the actuator is in the horizontal shearing direction.

Measuring equipment consists of two LVDTs to measure the vertical and horizontal displacements, two load cells (10

and 12) and two uniaxial accelerometers to measure vertical and horizontal vibrational accelerations on the soil sample. One of the accelerometers is mounted on top of the loading plate to measure vertical vibrational accelerations and the other accelerometer is attached to the top half of the shear box in the direction of shearing to measure horizontal vibrational accelerations. The output signals are collected by a NI CompactDAQ System, which in turn is connected to a PC to record the data with NI LabVIEW software.

The testing procedures basically follow ASTM D3080/D3080M (Standard Test Method for Direct Shear Test of Soils under Consolidated Drained Conditions). The change in testing procedures includes the application of vibration close to the end of a test when the soil sample reaches the critical state. Vibration is applied while the sample is being sheared. Frequency and force of the vibration are adjusted to a certain level and then kept constant.

#### 4 Tested materials

To evaluate the effect of vibration on the residual strength of granular material, four different dry granular materials (a total of 80 samples) were tested. The materials were 0.1 and 0.55 mm glass beads, as well as fine and coarse sands. These materials were selected to investigate the effect of particle shape and size on the vibro-residual strength characteristics at different vibrational accelerations. Particularly, different sizes of glass beads (0.1 and 0.55 mm) were chosen to check how different inertial forces (due to different size particles), generated among particles by vibration, contribute to the vibro-residual strength. On the other hand, coarse sand (well-rounded) and fine sand (angular) samples were chosen

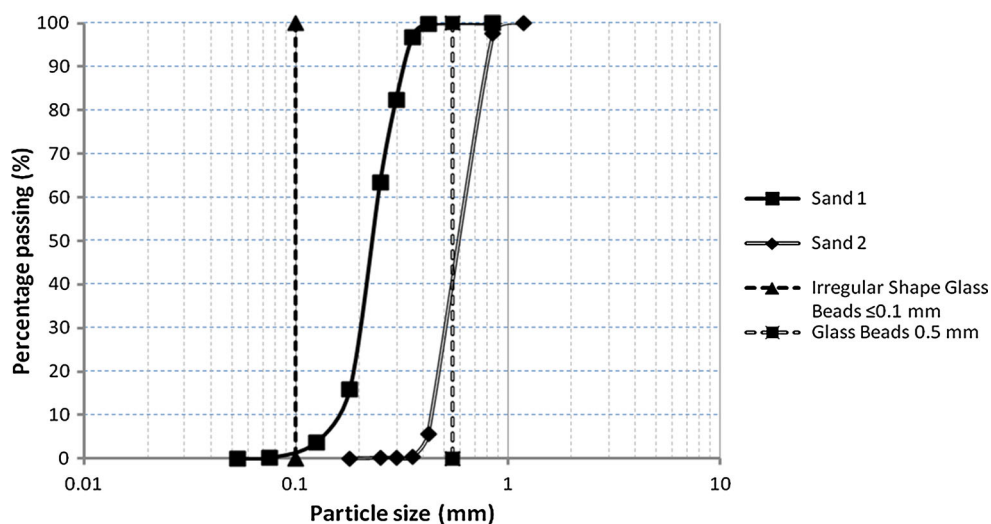


**Fig. 3** Particle size distribution of the materials tested (note that the plot of irregular shape glass beads does not show the actual particle size distribution of the material, but rather its upper size limit)

**Fig. 4** Pictures of the glass beads and sand under a microscope with  $\times 50$  magnification. **a** 0.1 mm glass beads; **b** 0.55 mm glass beads; **c** fine sand and **d** coarse sand

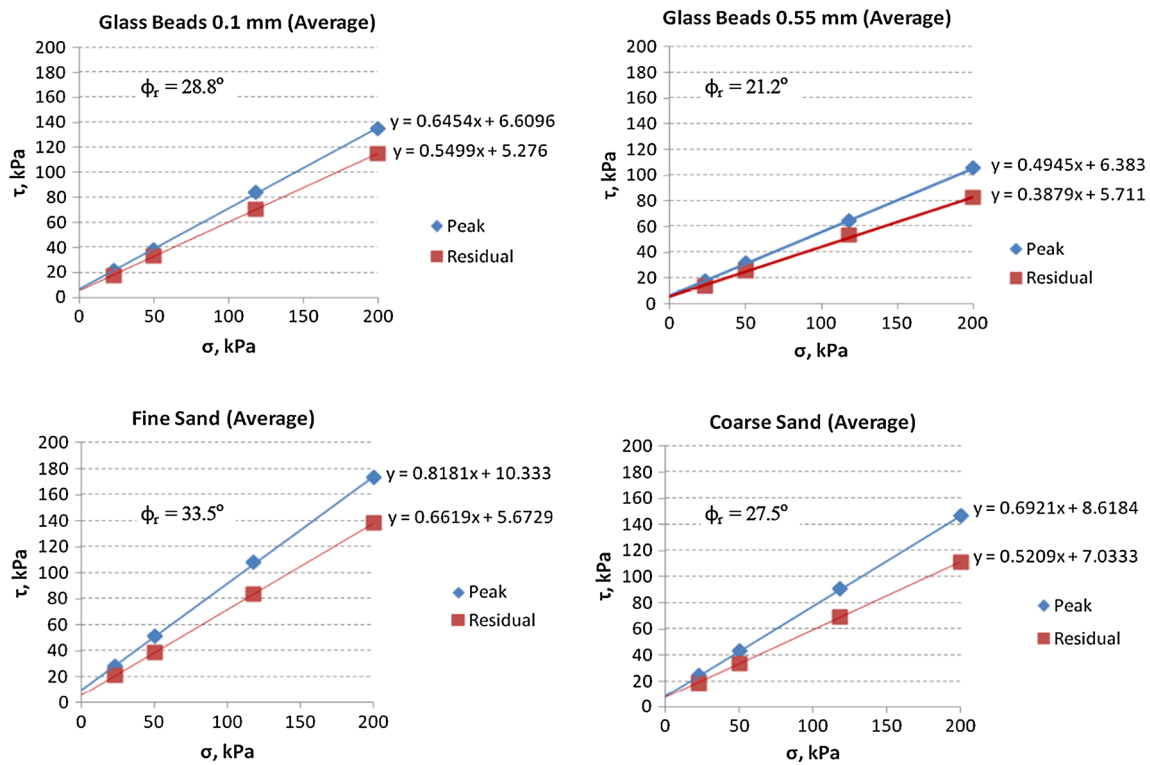
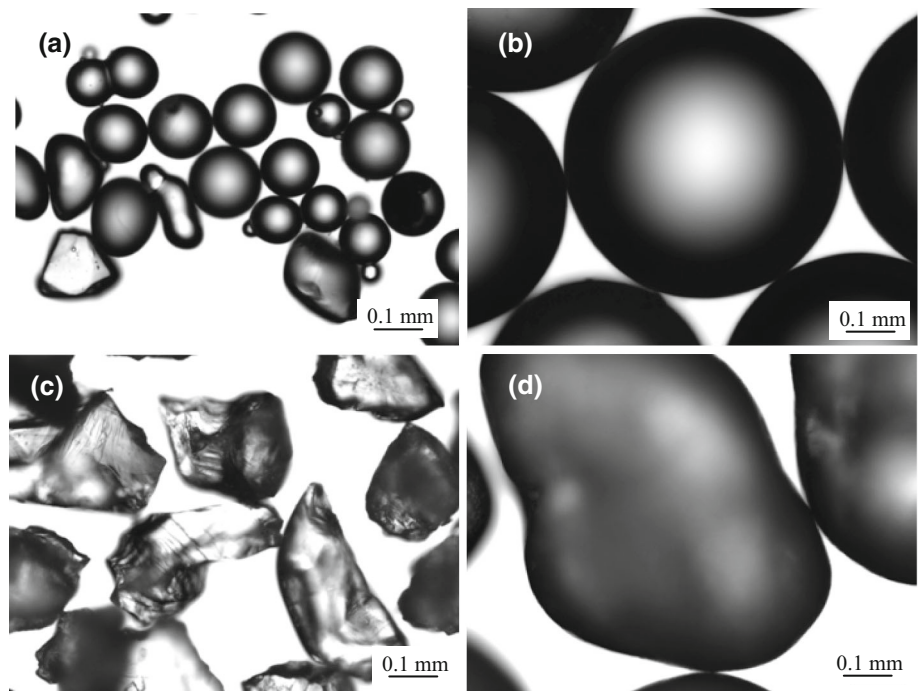


**Fig. 5** Shear strength diagrams of 0.1 mm glass beads, 0.55 mm glass beads, fine and coarse sands ( $\phi_r$ —residual friction angle)

**Table 2** Test results of 0.1 mm glass beads

Vibrational force (N)	Normal stress ( $\sigma$ kPa)	Peak strength ( $\tau_p$ kPa)	Residual strength ( $\tau_f$ kPa)	Vib.-Res. strength ( $\tau_{fd}$ kPa)	Vertical acceleration (g)	Horizontal acceleration (g)	Strength loss ( $\Delta \tau$ kPa)
1.61	23	21	19.5	18	0.03	0.1	1.5
	50	38.5	35	33	0.03	0.11	2
	118	82.5	71	68	0.04	0.12	3
	200	137.5	113	109.5	0.04	0.12	3.5
3.22	23	21	16.5	15	0.09	0.22	1.5
	50	38.5	29	26.5	0.08	0.23	2.5
	118	83.5	67	63	0.07	0.22	4
	200	135.5	114	108	0.065	0.2	6
3.71	23	21	18	15.5	0.075	0.25	2.5
	50	38	31.5	28	0.09	0.28	3.5
	118	85.5	70	65	0.08	0.24	5
	200	132	111.5	105	0.07	0.23	6.5
5.18	23	21.5	17	14	0.11	0.42	3
	50	38	32.5	26	0.11	0.38	6.5
	118	84	73	63	0.105	0.325	10
	200	136	121	108	0.09	0.3	13
7.14	23	22	17	13	0.14	0.5	4
	50	39.5	36	26.5	0.13	0.43	9.5
	118	83.5	73	56	0.15	0.43	17
	200	135	115	94	0.13	0.38	21

**Table 3** Test results of 0.55 mm glass beads

Vibrational force (N)	Normal stress ( $\sigma$ kPa)	Peak strength ( $\tau_p$ kPa)	Residual strength ( $\tau_f$ kPa)	Vib.-Res. strength ( $\tau_{fd}$ kPa)	Vertical acceleration (g)	Horizontal acceleration (g)	Strength loss ( $\Delta \tau$ kPa)
1.61	23	17.5	13.5	12.5	0.04	0.11	1
	50	32	25.5	24	0.035	0.11	1.5
	118	69	55.5	53.5	0.035	0.08	2
	200	111	82	79	0.035	0.09	3
3.22	23	17	14	12.5	0.07	0.175	1.5
	50	30.5	24.5	22.5	0.07	0.175	2
	118	65	51.5	47.5	0.07	0.175	4
	200	101	84	78	0.07	0.17	6
3.71	23	18	14	11.5	0.1	0.28	2.5
	50	32	25.5	22.5	0.085	0.23	3
	118	64	54	48.5	0.09	0.23	5.5
	200	103	82	73	0.085	0.23	9
5.18	23	17	14	10.5	0.105	0.325	3.5
	50	31	25.5	21	0.105	0.325	4.5
	118	62.5	51.5	43	0.105	0.325	8.5
	200	106	81	68	0.09	0.325	13
7.14	23	18	13.5	9	0.16	0.46	4.5
	50	32.5	25	19	0.16	0.46	6
	118	61.5	53	42	0.16	0.42	11
	200	106	83	66.5	0.14	0.43	16.5

**Table 4** Test results of fine sand

Vibrational force (N)	Normal stress ( $\sigma$ kPa)	Peak strength ( $\tau_p$ kPa)	Residual strength ( $\tau_f$ kPa)	Vib.-Res. strength ( $\tau_{fd}$ kPa)	Vertical acceleration (g)	Horizontal acceleration (g)	Strength loss ( $\Delta \tau$ kPa)
1.61	23	27	21	19.5	0.045	0.15	1.5
	50	53.5	40	38	0.045	0.12	2
	118	110	87.5	85.5	0.05	0.12	2
	200	178.5	139	137	0.045	0.11	2
3.22	23	26.5	20.5	17.5	0.1	0.26	3
	50	49	38.5	35	0.1	0.27	3.5
	118	107.5	83	77.5	0.09	0.27	5.5
	200	170.5	137.5	131	0.07	0.23	6.5
3.71	23	30	22	18.5	0.09	0.25	3.5
	50	51.5	37	33.5	0.1	0.27	3.5
	118	107.5	81	75	0.09	0.27	6
	200	169	143	134.5	0.08	0.25	8.5
5.18	23	29.5	22	17.5	0.1	0.37	4.5
	50	51	39.5	33.5	0.115	0.38	6
	118	108.5	82.5	71.5	0.105	0.37	11
	200	171	134	121	0.1	0.32	13
7.14	23	30	21	14.5	0.17	0.5	6.5
	50	50.5	37.5	27.5	0.155	0.49	10
	118	108	83	65	0.145	0.47	18
	200	177	138	116	0.145	0.45	22

**Table 5** Test results of coarse sand

Vibrational force (N)	Normal stress ( $\sigma$ kPa)	Peak strength ( $\tau_p$ kPa)	Residual strength ( $\tau_f$ kPa)	Vib.-Res. strength ( $\tau_{fd}$ kPa)	Vertical acceleration (g)	Horizontal acceleration (g)	Strength loss ( $\Delta \tau$ kPa)
1.61	23	25	18.5	17	0.045	0.12	1.5
	50	42	34.5	33	0.04	0.12	1.5
	118	88.5	67.5	66	0.045	0.1	1.5
	200	145	108.5	106.5	0.04	0.1	2
3.22	23	24.5	18.5	16.5	0.075	0.2	2
	50	43	34	31.5	0.065	0.2	2.5
	118	89	67.5	64.5	0.07	0.19	3
	200	145.5	111	107	0.07	0.18	4
3.71	23	24	18.5	16	0.085	0.23	2.5
	50	44.5	33.5	30.5	0.075	0.22	3
	118	93.5	70	66.5	0.075	0.21	3.5
	200	148.5	116	111	0.075	0.2	5
5.18	23	24	18	14.5	0.12	0.35	3.5
	50	43	34.5	29.5	0.09	0.33	5
	118	91.5	71	65.5	0.1	0.28	5.5
	200	148	110	102	0.08	0.28	8
7.14	23	23.5	18	12	0.2	0.59	6
	50	44.5	32	25.5	0.145	0.4	6.5
	118	91	68.5	59	0.135	0.39	9.5
	200	147	109	95	0.1	0.39	14

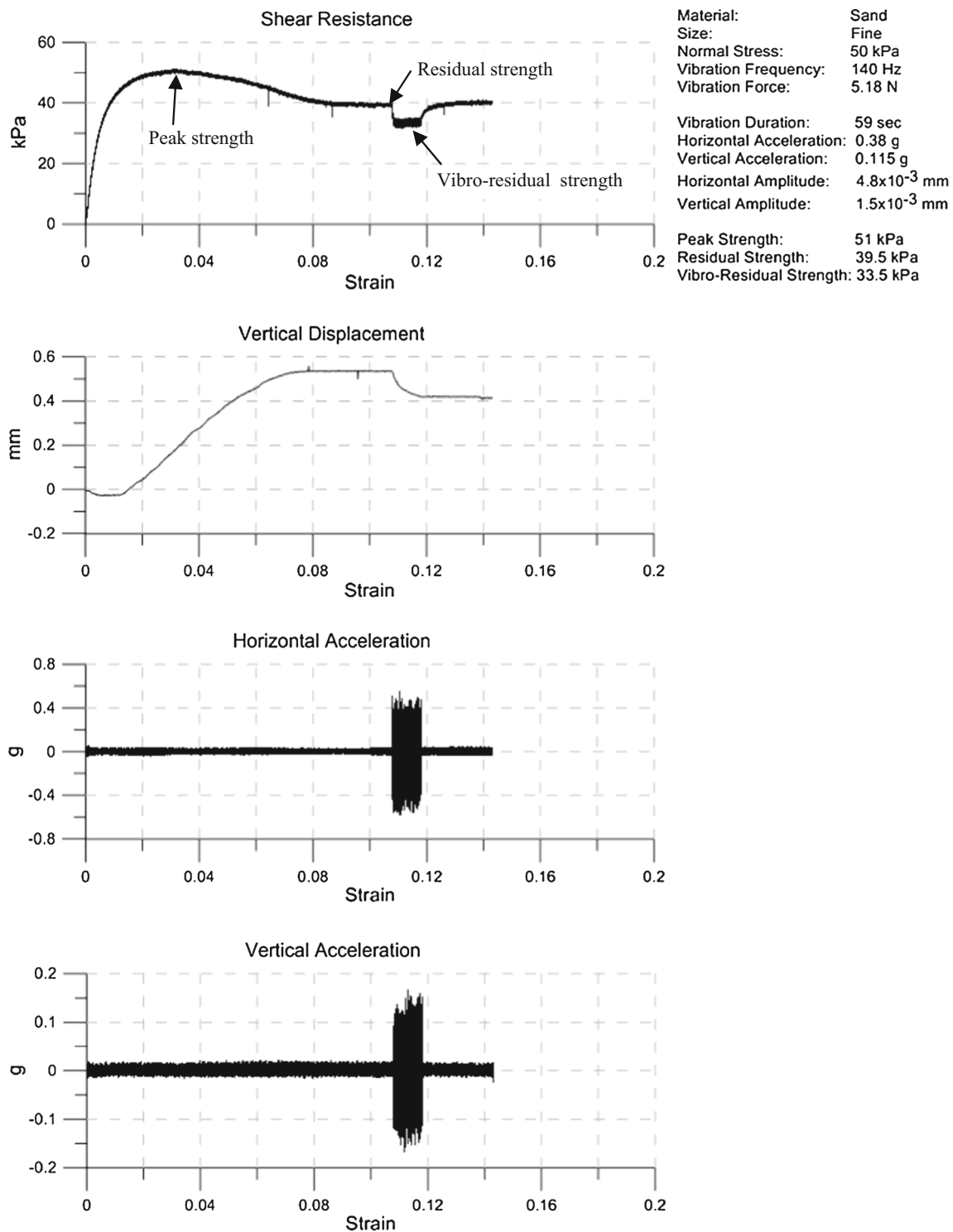


**Fig. 6** Shear stress, vertical displacement, horizontal and vertical accelerations versus strain of fine sand subjected to a normal stress of  $\sigma = 50$  kPa, 140 Hz vibration frequency and 5.18 N vibration force

in addition to the glass beads in order to evaluate the effect of particle roundness on vibro-residual strength of the materials, particularly, to observe the influence of particle friction during the induced vibration.

The samples [6 cm  $\times$  6 cm  $\times$  3.2 cm (W  $\times$  L  $\times$  H) in size] were tested at 23, 50, 118 and 200 kPa normal stresses in strain-controlled mode at a shear rate of 0.61 mm/min. A vibration frequency of 140 Hz was used in all samples.



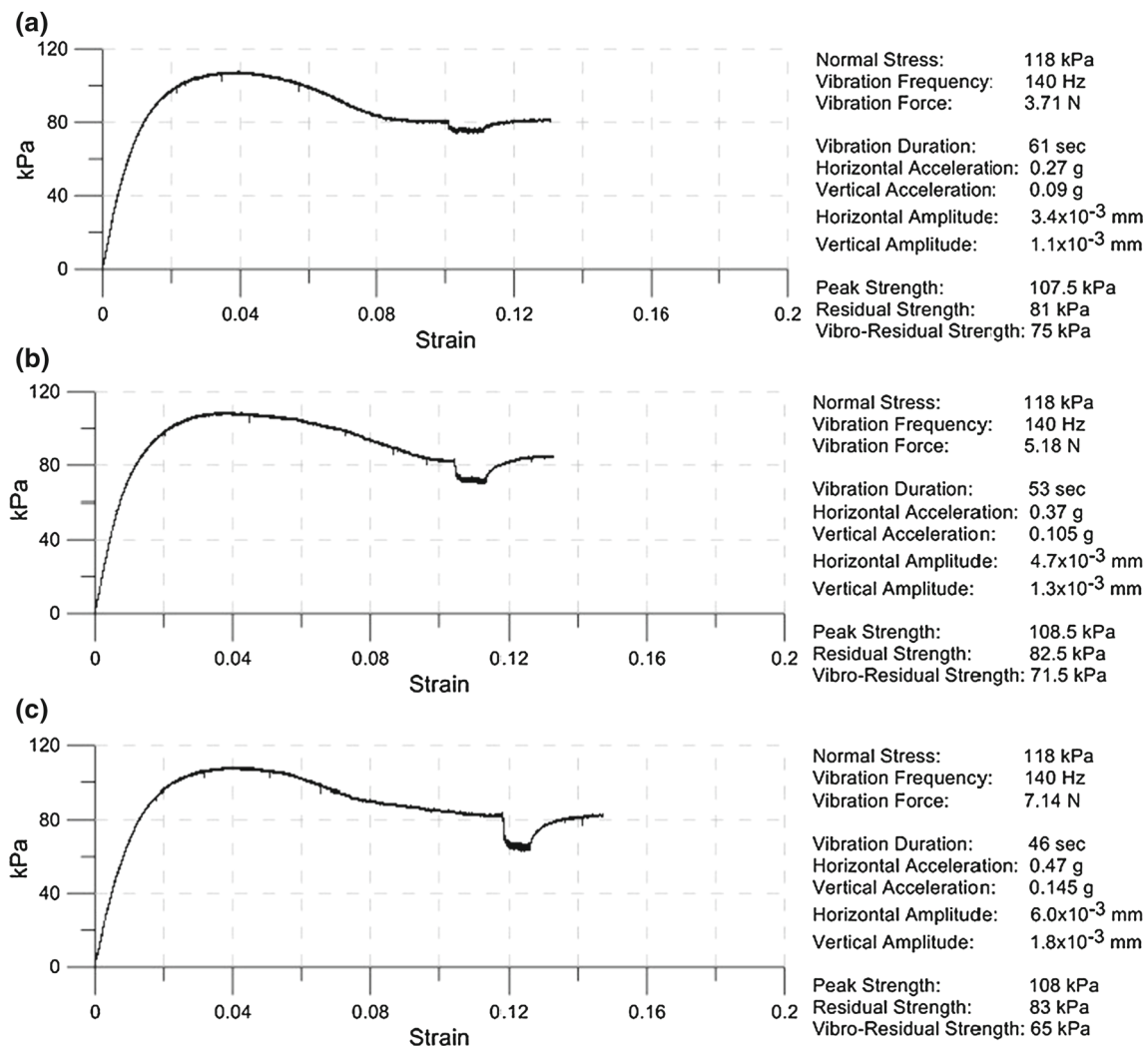


**Fig. 7** Shear stress plots of three fine sand samples tested at 118 kPa normal stress and different vibration accelerations

From each type of granular material five sets of samples (four samples in each set) were tested at five different vibration intensities. The maximum impact forces of the actuator electromagnets were 1.61, 3.22, 3.71, 5.18 and 7.14 N. Note that these impact forces are the designed forces provided by actuator. The actual impact forces may vary during the test. They were measured by the accelerometers and load cell. All data was recorded at a rate of 1 kHz.

The physical characteristics of the tested materials are provided in Table 1. The particle size distributions of the four materials are given in Fig. 3. Representative samples of the materials were examined under a microscope to determine the shape of the particles (see Fig. 4a–d). It is seen in Fig. 4a that the 0.1 mm glass beads contain significant amount of irregular shape grains and some beads are smaller than 0.1 mm. Therefore, the “0.1 mm glass beads” should be treated as a mixture of fine sand and glass beads with 0.1 mm and smaller sizes. The 0.55 mm glass beads are basi-

cally ideal spherical shape (see Fig. 4b). From Fig. 4c–d it can be seen that the fine sand particles have angular shape and the coarse sand is well rounded. The shear strength diagrams and the residual friction angles of the four materials are shown in Fig. 5.

## 5 Test results under vibrations

Summary of the test results of 0.1 mm glass beads, 0.55 mm glass bead, fine and coarse sands are given in Tables 2, 3, 4 and 5, respectively. Figure 6 shows a typical plot of shear stress, vertical displacement, horizontal and vertical accelerations versus strain of fine sand. Shearing resistance of the material was measured using a load cell mounted at the top half of the shear box [see Fig. 1b (12)]. Vertical displacements were measured from an LVDT attached to the loading plate of the shear box. Horizontal and vertical accel-

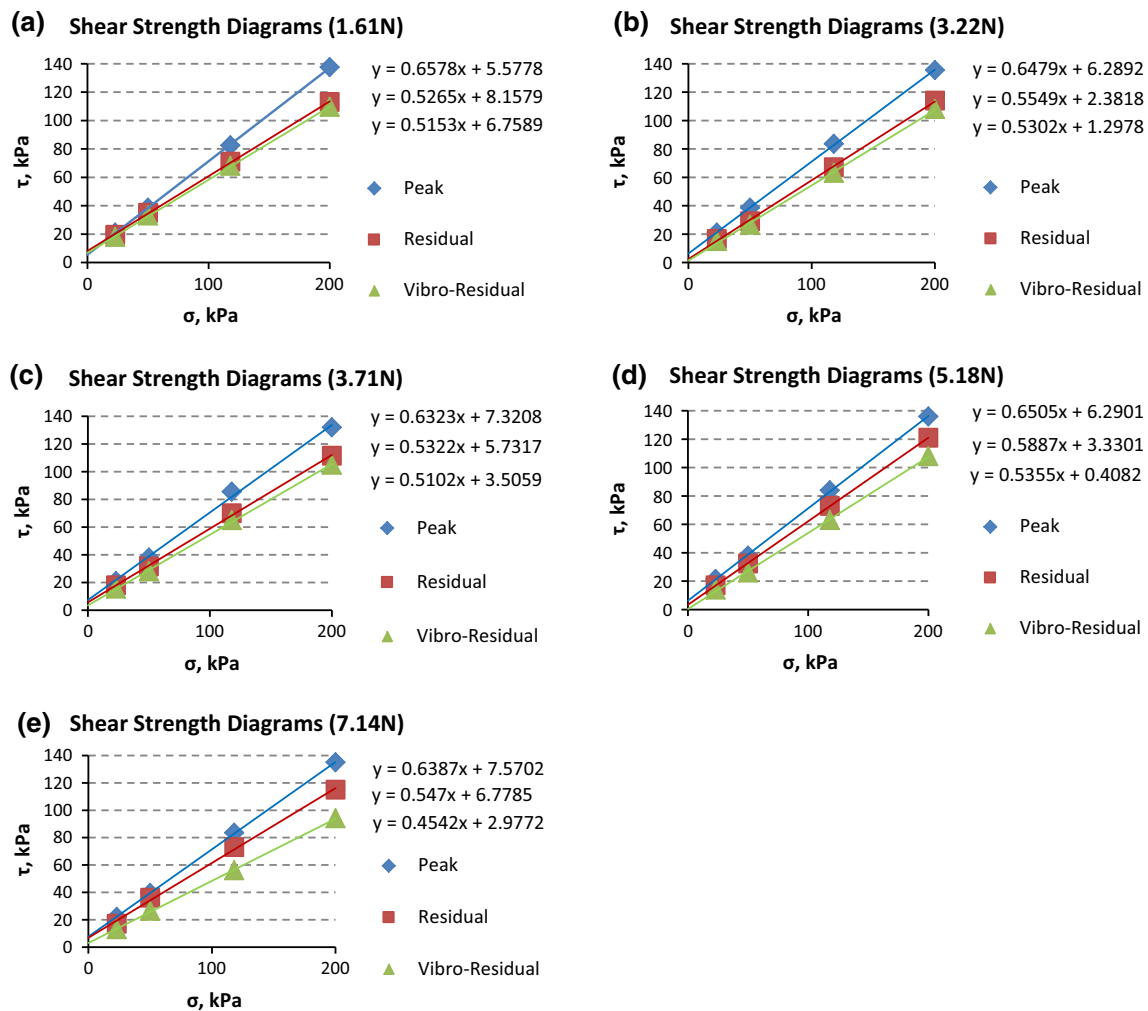


**Fig. 8** Shear strength envelopes of 0.1 mm glass beads tested at: **a** 1.61 N vibration force; **b** 3.22 N vibration force; **c** 3.71 N vibration force; **d** 5.18 N vibration force and **e** 7.14 N vibration force

erations were obtained from an accelerometer attached to the top half of the shear box in the direction of shearing and a second accelerometer measuring vertical accelerations of the loading plate, respectively. All data except vertical displacement were collected at a rate of 1 kHz. Due to the technical characteristics of the LVDT, vertical displacements were measured at a rate of 2 Hz filtered from an original rate of 1 kHz.

As seen in Fig. 6, vibration was applied when the soil reached the critical state. The shear resistance plot shows that during vibration there is an immediate strength loss  $\Delta \tau$  from residual to vibro-residual state. The vibro-residual strength remains practically constant during vibration. When vibration is terminated the shear strength of the material gradually increases and reaches the quasi-static residual strength value.

All the samples have experienced contraction, decrease in volume, due to vibration as shown in the vertical displace-

ment plot in Fig. 6. It is seen that contraction takes place during vibration and the volume change is permanent or plastic. The initial volume before vibration cannot be restored when vibration stops.

An example of the effect of an increase in horizontal vibration acceleration on the residual shear strength of fine sand is provided in Fig. 7a–c, which shows the plots of fine sand samples tested at 3.71, 5.18 and 7.14 N vibrational forces of electromagnets and 0.27, 0.37 and 0.47 g horizontal accelerations, respectively. The example demonstrates that at constant normal stress (118 kPa) and vibration frequency an increase in vibration acceleration by 0.1 g results in greater strength loss.

The peak, residual and vibro-residual shear strength envelopes of 0.1 and 0.55 mm glass beads, as well as fine and coarse sand at five different vibration forces are shown in Figs. 8, 9, 10 and 11, respectively. The peak, residual and vibro-residual friction angles of the four materials are given

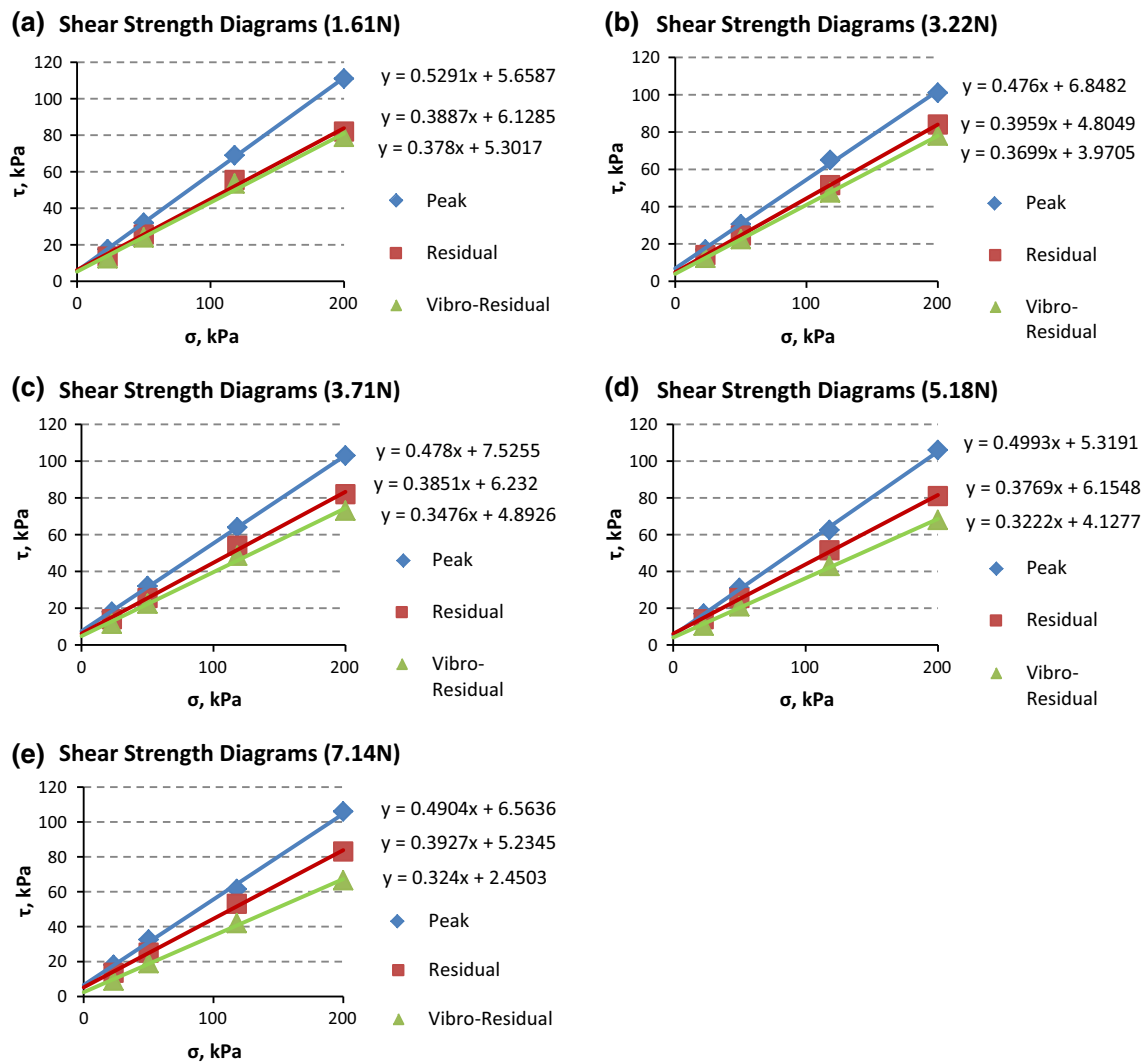


**Fig. 9** Shear strength diagrams of 0.55 mm glass beads tested at: **a** 1.61 N vibration force; **b** 3.22 N vibration force; **c** 3.71 N vibration force; **d** 5.18 N vibration force and **e** 7.14 N vibration force

in Tables 6, 7, 8 and 9. As seen in Figs. 8, 9, 10 and 11 and acceleration values in Tables 2, 3, 4 and 5, increase in the vibration force results in an increase of vertical and horizontal accelerations and amplitudes (not provided in Table 2, 3, 4, 5), which in turn results in a greater loss in residual strength at a given normal stress. From the tables and figures it is seen that vibration decreases the residual friction angle.

It should be mentioned that all the samples tested have experienced compression due to the applied vibration, which correlates well with the experimental results obtained by Youd [38]. It is interesting to note that after the termination of vibration no change in vertical displacement (void ratio) has been observed. On the other hand, the post-vibrational shear resistance increases from vibro-residual strength back to the residual strength value before applying vibration. This implies that the compression of the specimens caused by

vibration did not affect the actual shear zones, otherwise an increase in shear stress, greater than the static residual strength, would have been observed in post-vibrational shear behaviour [34].

### 5.1 The effect of strength loss due to changes in normal stress caused by vibration

Changes in the shearing resistance can be due to changes in the normal stress during vibration, Maslov [15]. In this study, vertical acceleration has been measured in order to calculate the normal stress acting on a sample during vibration. From Newton's Second Law of Motion ( $F = ma$ ), knowing the vertical acceleration of the loading plate and the mass acting on the loading plate, the force due to vibration can be calculated. Using the area ( $A$ ) of the sample, the reduction in normal stress can be calculated from  $\Delta\sigma = F/A$ . Knowing the  $\Delta\sigma$

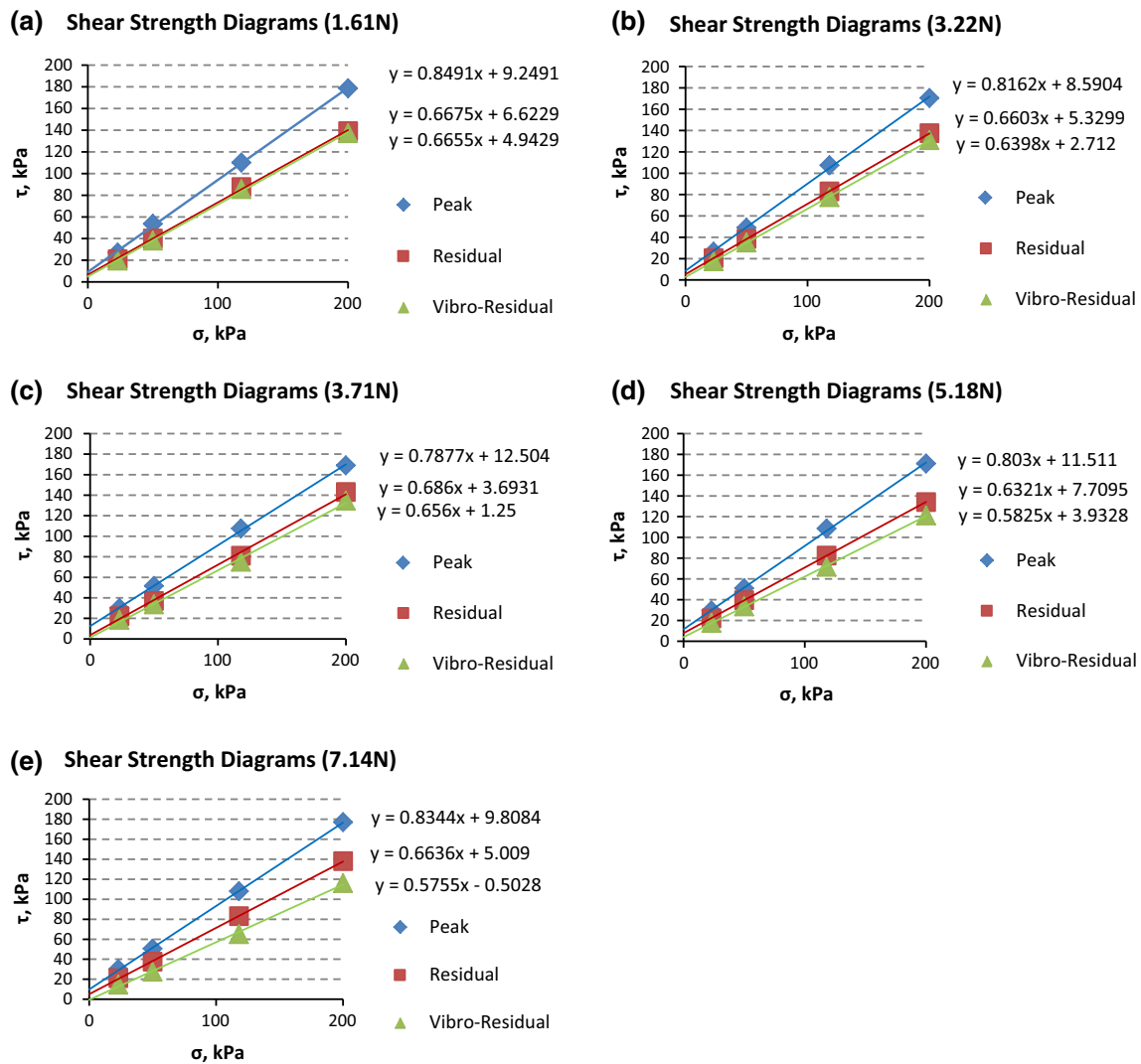


**Fig. 10** Shear strength diagrams of fine sand tested at: **a** 1.61 N vibration force; **b** 3.22 N vibration force; **c** 3.71 N vibration force; **d** 5.18 N vibration force and **e** 7.14 N vibration force

value and using the residual shear strength diagram (equation) of the material, the strength loss  $\Delta \tau'$  due to reduced normal stress  $\Delta \sigma$  is obtained.

The measured total residual strength loss  $\Delta \tau$  and the calculated residual strength loss  $\Delta \tau'$  due to the normal stress reduction caused by vibration are provided in Figs. 12, 13, 14 and 15, where  $\Delta \tau$  is equal to the total strength loss,  $\Delta \tau'$  is the strength loss due to reduction in normal stress  $\sigma$ , for samples tested at normal stresses of  $\sigma = 23, 50, 118$  and  $200$  kPa, denoted by 1, 2, 3 and 4 respectively in the figures.

As seen in Figs. 12, 13, 14 and 15 the residual strength loss  $\Delta \tau'$  due to a reduction in normal stress  $\Delta \sigma$  caused by vibration for the all materials are very small compared to the total strength loss  $\Delta \tau$ . Therefore, it can be concluded that although there is some reduction in normal stress due to vibration, the contribution to the loss in residual strength is

minimal and the strength loss is mainly due to the material fluidization.

## 5.2 The effects of accelerations on residual strength loss

Based on the data from Tables 2, 3, 4 and 5, the total residual strength loss are plotted against horizontal acceleration for 0.1 mm glass beads, 0.55 mm glass beads, fine sand and coarse sand and the results are shown in Figs. 16, 17, 18, and 19. As seen in Figs. 16, 18 and 19 the effect of horizontal acceleration on the strength loss for 0.1 mm glass beads, fine and coarse sand is nonlinear under higher normal stresses of 50, 118 and 200 kPa. The relationship is practically linear at low normal stress of  $\sigma = 23$  kPa. Also the plots become more nonlinear with the increase in the normal stress from 50 to 200 kPa. On the other hand, Fig. 17 shows that the strength loss versus horizontal acceleration relationship for 0.55 mm

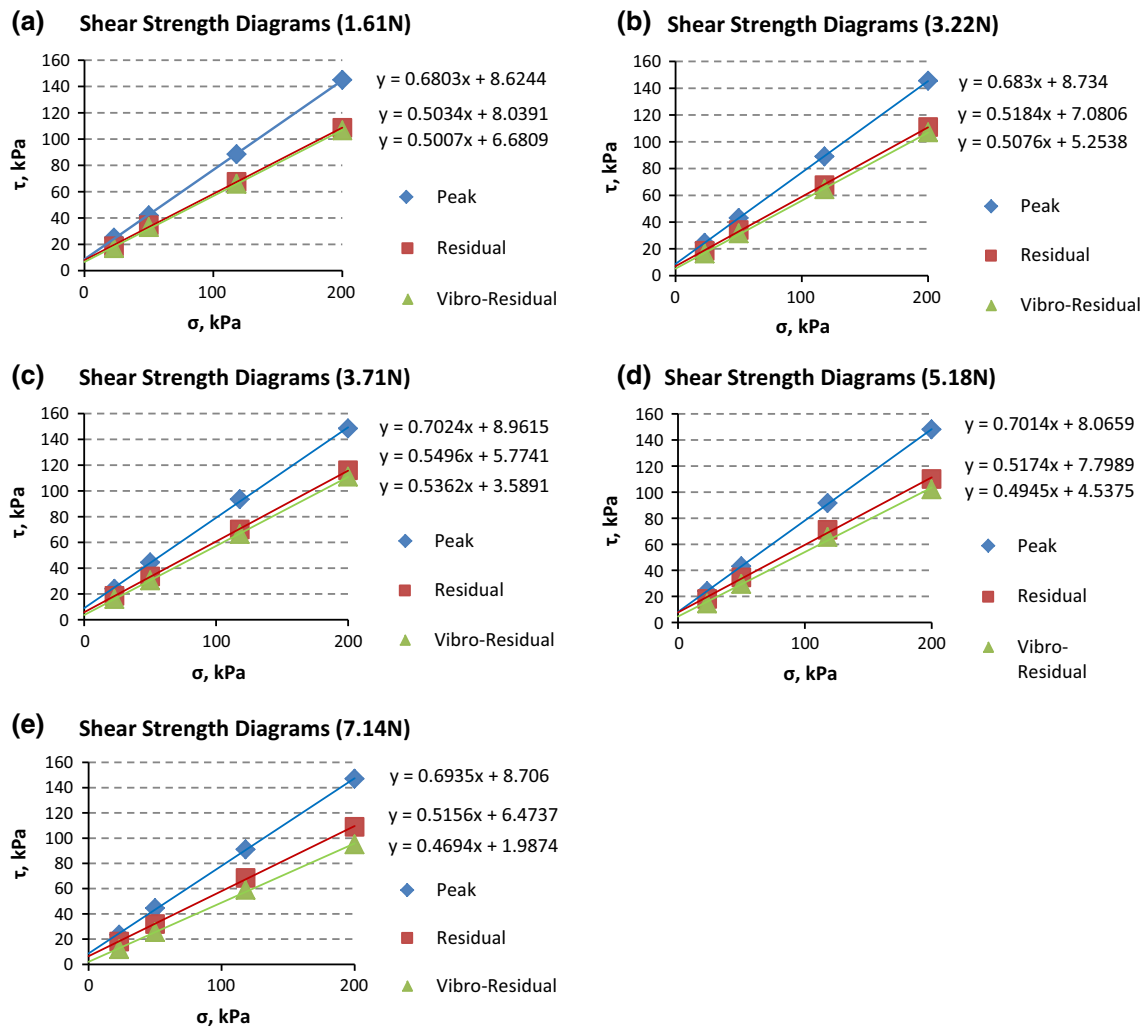


**Fig. 11** Shear strength diagrams of coarse sand tested at: **a** 1.61 N vibration force; **b** 3.22 N vibration force; **c** 3.71 N vibration force; **d** 5.18 N vibration force and **e** 7.14 N vibration force

glass beads is practically linear under all normal stress values (23, 50, 118 and 200 kPa). This can probably be explained by the absence of irregular shape particles in this material (see Fig. 4b). It has been discussed earlier that the 0.1 mm glass beads were not round which consisted of angular and irregular particles. It can be considered as a mixture of fine angular sand and glass beads having size up to 0.1 mm in diameter.

As it was mentioned above the irregular shape of particles comprising the tested 0.1 mm glass beads, fine and coarse sands results in nonlinearity of horizontal acceleration versus residual strength loss diagrams at higher normal stresses (50, 118 and 200 kPa). It is apparent from Figs. 16, 18 and 19 that unlike the plots of samples tested at 23 kPa normal stress, the samples tested at higher normal stress values demonstrate less strength loss at low horizontal accelerations than they would do if their plots were linear. This phenomenon can be explained by the additional friction among particles

**Table 6** Friction angles of 0.1 mm glass beads

Vibrational force (N)	$\varphi(^{\circ})$		
	Peak	Residual	Vibro-residual
1.61	33.3	27.8	27.3
3.22	32.9	29	27.9
3.71	32.3	28	27
5.18	33	30.5	28.2
7.14	32.6	28.7	24.4

due to their irregular shapes. The irregular shape of particles generates greater shear resistance during their rotational and translational motions induced by relatively low vibration intensities.

On the other hand 0.55 mm glass beads have practically round shape and unlike the other materials they do not generate additional friction due to the irregular shape of the grains.

**Table 7** Friction angles of 0.55 mm glass beads

Vibrational force (N)	$\phi(^{\circ})$		
	Peak	Residual	Vibro-residual
1.61	27.9	21.2	20.7
3.22	25.5	21.6	20.3
3.71	25.5	21.1	19.2
5.18	26.5	20.7	17.9
7.14	26.1	21.4	17.9

**Table 8** Friction angles of fine sand

Vibrational force (N)	$\phi(^{\circ})$		
	Peak	Residual	Vibro-residual
1.61	40.3	33.7	33.6
3.22	39.2	33.4	32.6
3.71	38.2	34.5	33.3
5.18	38.8	32.3	30.2
7.14	39.8	33.6	29.9

**Table 9** Friction angles of coarse sand

Vibrational force (N)	$\phi(^{\circ})$		
	Peak	Residual	Vibro-residual
1.61	34.2	26.7	26.6
3.22	34.3	27.4	26.9
3.71	35.1	28.8	28.2
5.18	35	27.4	26.3
7.14	34.7	27.3	25.1

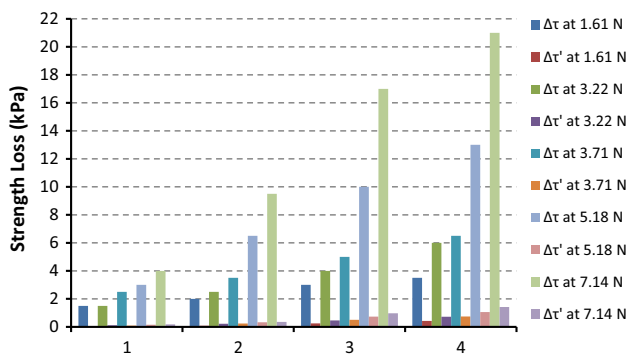


**Fig. 12** Total strength loss and strength loss due to reduced normal stress for 0.1 mm glass beads

Here the round shape of the particles results in linear pattern of the horizontal acceleration versus residual strength loss plots at all normal stress values (23, 50, 118 and 200 kPa) as it is seen in Fig. 17.

It should also be noted that at higher horizontal acceleration strength loss of 0.1 mm glass beads, fine and coarse sand

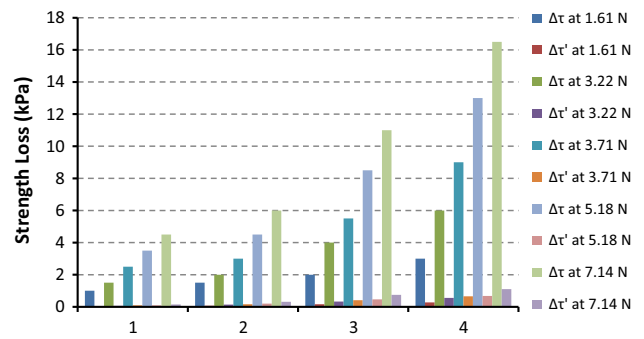


**Fig. 13** Total strength loss and strength loss due to reduced normal stress for 0.55 mm glass beads

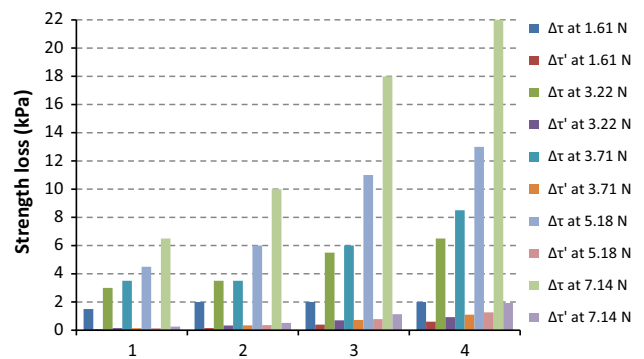


**Fig. 14** Total strength loss and strength loss due to reduced normal stress for fine sand

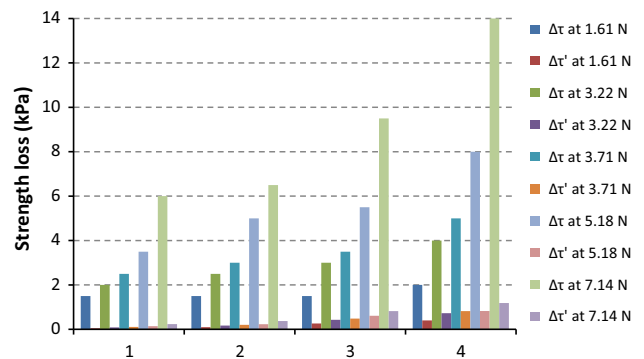


**Fig. 15** Total strength loss and strength loss due to reduced normal stress for coarse sand

samples increases notably. This implies that there is a certain value of horizontal acceleration above which the effect of irregular shape of the particles becomes insignificant.

Figures 16, 17, 18 and 19 can be used to estimate the strength loss due to vibration for different normal stresses and accelerations.

## 6 Conclusions

A new experimental technique and apparatus have been introduced in this paper to study the effect of vibration on the

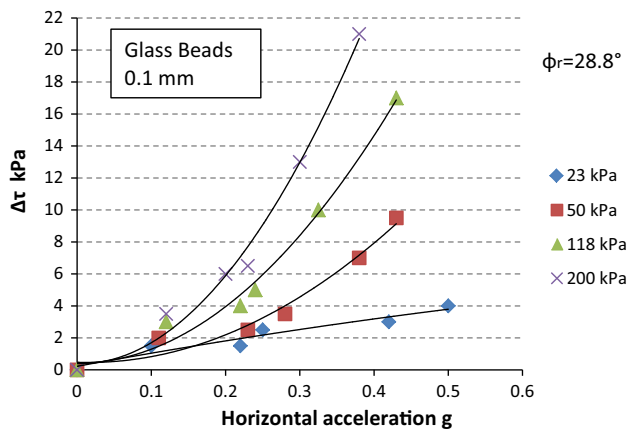


**Fig. 16** Total strength loss ( $\Delta \tau$ ) versus horizontal acceleration of 0.1 mm glass beads

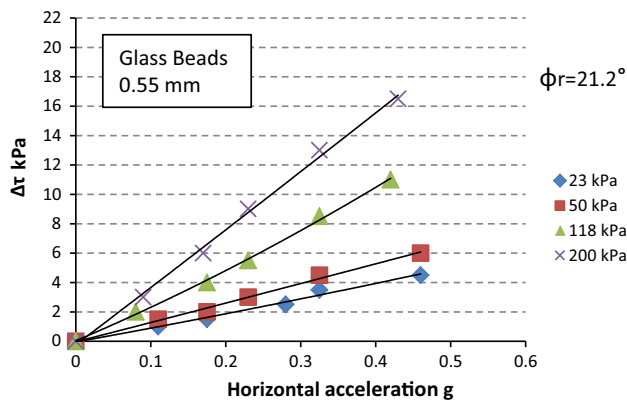


**Fig. 17** Total strength loss ( $\Delta \tau$ ) versus horizontal acceleration of 0.55 mm glass beads

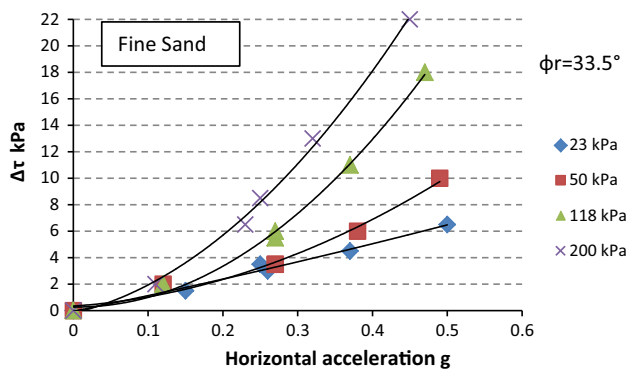


**Fig. 18** Total strength loss ( $\Delta \tau$ ) versus horizontal acceleration of fine sand

critical state strength of granular material. If the material is subjected to vibration after reaching the critical state, there is a decrease in volume and shearing resistance of the material. A decrease in volume implies compaction and denser state which usually leads to higher shear strength in under static condition. However the shearing resistance of the material is reduced during vibration. Based on the test results of 0.1 and

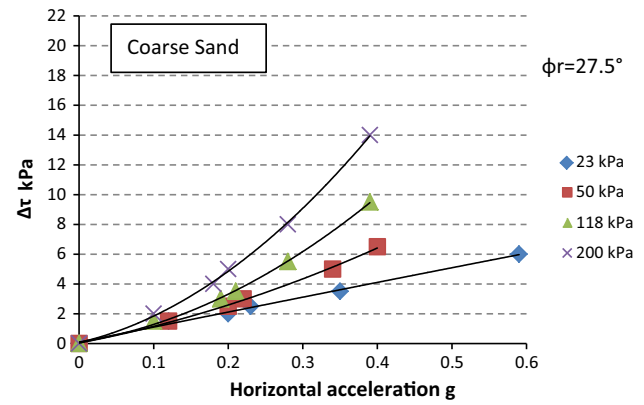


**Fig. 19** Total strength loss ( $\Delta \tau$ ) versus horizontal acceleration of coarse sand

0.55 mm glass beads and fine and coarse sands, the following conclusion can be made:

1. Upon application of a sufficiently strong vibration at the critical strength state of a granular material, an immediate strength loss takes place from residual to vibro-residual strength, after which the vibro-residual strength remains practically constant during vibration.
2. Vibration does not have any permanent post-vibrational effects on the residual strength of granular material, provided that there is sufficient shear displacement of the material after termination of the vibration.
3. Initially dense or loose granular material compresses when vibration is applied at its critical strength state.
4. At a constant vibration frequency, an increase in vibration force results in an increase in the vertical and horizontal vibration accelerations and amplitudes, which in turn results in a larger residual strength loss at the given normal stress.
5. Sufficiently strong vibration lowers the residual friction angle, that is, the residual strength loss magnitude increases with an increase in the normal stress.
6. Residual strength loss  $\Delta \tau$  due to the normal stress reduction caused by vibration for the all granular materials being tested is small compared to the total loss in residual strength  $\Delta \tau$ . Therefore, it can be concluded that although normal stress reduction caused by vibration (in the given range of accelerations) contributes to the residual strength loss, the strength loss is mainly due to material fluidization.
7. For a given test condition, the relationship between the residual strength loss and horizontal acceleration is non-linear for irregularly shaped particles. The nonlinearity increases with an increase in confining (normal) stress.
8. For a given test condition, the relationship between the residual strength loss and horizontal acceleration is linear for glass beads (0.55 mm) with spherical shape particles under all normal stresses being tested.

**Acknowledgments** Financial support of this project was provided by the Natural Science and Engineering Council of Canada (NSERC), the NSERC Postgraduate Scholarship and the Alberta Innovates Graduate Student Scholarship. The project was performed in the Department of Civil and Environmental Engineering at the University of Alberta.

## References

- Bagnold, R.A.: Experiments on the gravity-free dispersion of large solid spheres in a Newtonian fluid under shear. *Proc. R. Soc. Lond.* **225**, 49–63 (1954)
- Barkan, D.D.: *Dynamics of Basis and Foundations* (Transl from Russian by L. Drashevskaya). McGraw-Hill, New York (1962)
- Bjerrum, L., Kringstad, S., Kummeneje, O.: The Shear Strength of a Fine Sand. In: *Proceedings of the 5th international conference on soil mechanics and foundation engineering*, pp. 29–37 (1961)
- Bougie, J.Lee: *Continuum Simulations of Fluidized Granular Materials*. The University of Texas, Austin (2004)
- Das, B.M.: *Principles of Soil Dynamics*, 2nd edn. Cengage Learning, Stamford (2011)
- Davies, T.R.H.: Spreading of rock avalanche debris by mechanical fluidization. *Rock Mech.* **15**, 9–24 (1982)
- Dijksman, J.A., Wortel, G.H., van Dellen, L.T.H., Dauchot, O., van Hecke, M.: Jamming, yielding, and rheology of weakly vibrated granular media. *Phys. Rev. Lett.* **107**, 108303 (2011)
- Housner, G.W.: Geotechnical problems of destructive earthquakes. *Geotechnique*. **4**(4), 153–162 (1954)
- Housner, G.W.: Behavior of structures during earthquakes. *J. Eng. Mech. Div. ASCE* **85**(4), 109–129 (1959)
- Huan, C.: NMR experiments on vibrofluidized and gas fluidized granular systems. Ph.D. Thesis, University of Massachusetts Amherst (2008)
- Hung, O.: Dynamics of rock avalanches and other types of slope movements. Ph.D. Thesis, University of Alberta (1981)
- Idriss, I.M., Boulanger, R.W.: *Soil Liquefaction During Earthquakes*. Earthquake Engineering Research Institute, Oakland (2008)
- Ingale, R.A.: Dynamics of vibrated granular matter. Ph.D. thesis, The City University of New York (2008)
- Jaeger, H.M., Nagel, S.R., Behringer, R.P.: Granular solids, liquids, and gases. *Rev. Mod. Phys.* **68**, 1259 (1996)
- Maslov, N.N.: Stability Conditions of Saturated Sands. (Russian: Usloviya Ustoychivosti Vodonasishennikh Peskov). Gosenergoizdat, Leningrad (1959)
- Meehan, C.L., Boulanger, R.W., Duncan, J.M.: Dynamic centrifuge testing of slickensided shear surfaces. *J. Geotech. Eng. Div. ASCE* **134**(8), 1086–1096 (2008)
- Melhus, M.F.: Effects of noise and vibration on the solid to liquid fluidization transition in small dense granular systems under shear. Ph.D. Thesis, Northwestern University, Evanston, Illinois (2011)
- Melosh, H.J.: Acoustic fluidization: a new geologic process? *J. Geophys. Res.* **84**, 7513–7520 (1979)
- Melosh, H.J.: Dynamical weakening of faults by acoustic fluidization. *Nature* **379**, 601–606 (1996)
- Metcalf, C., Tennakoon, S.G.K., Kondic, L., Schaeffer, D.G., Behringer, R.P.: Granular friction, Coulomb failure, and the fluid-solid transition for horizontally shaken granular materials. *Phys. Rev. E Stat. Nonlin. Soft Matter Phys.* **65**(3), 03130201–03130215 (2002)
- Pokrovsky, G.I., Ehrlich, A.A., Laletin, N.V., Lush, F.A.: New methods of investigation of the compressibility and internal friction in soils. *Vestnik Voenno-Inzhenernoy Akademii RKKA* **6** (1934)
- Pyke, R., Seed, H.B., Chan, C.K.: Settlement of sands under multi-directional shaking. *J. Geotech. Eng. Div. ASCE* **101**(4), 379–398 (1975)
- Richards Jr, R., Elms, D., Budhu, M.: Dynamic fluidization of soils. *J. Geotech. Eng.* **116**(5), 740–759 (1990)
- Richart, F.E.: *Vibrations of Soils and Foundations*. Prentice-Hall, Englewood Cliffs (1970)
- Robertson, P.K., Campanella, R.G.: Liquefaction potential of sands using the CPT. Research Report R69-15, Department of Civil Engineering, Massachusetts Institute of Technology, Cambridge, MA (1985)
- Robertson, P.K., Campanella, R.G.: Estimating liquefaction potential of sands using the flat plate dilatometer. *Geotech. Test. J.* **9**(1), 38–40 (1986)
- Sangroya, R., Choudhury, D.: Stability analysis of soil slope subjected to blast induced vibrations using FLAC3D. *Geo-Congress* **2013**, 472–481 (2013)
- Savchenko, I.A.: Effect of vibrations on internal friction in sand. In: *Symposium, Soil Dynamics, Moscow, Gosstroizdat, No. 2* (1958)
- Seed, H.B.: A method for earthquake resistant design of earth dams. *J. Soil Mech. Found. Div. ASCE* **92**(1), 13–41 (1966)
- Seed, H.B., Idriss, I.M.: *Ground Motions and Soil Liquefaction During Earthquakes*. Monograph. Earthquake Engineering Research Institute, Berkeley (1982)
- Seed, H.B., Idriss, I.M.: Evaluation of liquefaction potential using field performance data. *J. Geotech. Eng. ASCE* **109**(3), 458–482 (1983)
- Shibata, T., Yukitomo, H.: Liquefaction process of sand during cyclic loading. *Soils Found.* **3**, 54–69 (1969)
- Sornette, D., Sornette, A.: Acoustic fluidization for earthquakes? *Bull. Seismol. Soc. Am.* **90**(3), 781–785 (2000)
- Taslagyan, K.A., Chan, D.H., Morgenstern, N.R.: A direct shear apparatus with vibrational loading. *ASTM Geotech. Test. J.* **38**(1), 8 (2015)
- Wartman, J., Seed, R.B., Bray, J.D.: Shaking table modeling of seismically induced deformations in slopes. *J. Geotech. Geoenviron. Eng.* **131**(5), 610–622 (2005)
- Wassgren, C.R.: *Vibration of granular materials*. Ph.D. Thesis, California Institute of Technology, Pasadena, California (1997)
- Youd, L.T.: Reduction of critical void ratio during steady-state vibration. In: *Proceedings of international symposium on wave propagation and dynamic properties of earth materials, Albuquerque, N. Mex.*, pp. 737–744 (1967)
- Youd, L.T.: Densification and Shear of Sand during Vibration. *ASCE J. Soil Mech. Found. Div.* **96**(3), 863–880 (1970)